Electrostatic effects play a central role in cold adaptation of trypsin

Bjørn Olav Brandsdal[a], Arne O. Smalås[a], Johan Åqvist[b,*]

[a] *Department of Chemistry, Faculty of Science, University of Tromsø, N-9037 Tromsø, Norway*
[b] *Department of Cell and Molecular Biology, Uppsala University, Biomedical Centre, P.O. Box 596, S-75124 Uppsala, Sweden*

Received 3 April 2001; revised 18 May 2001; accepted 18 May 2001

First published online 1 June 2001

Edited by Matti Saraste

Abstract Organisms that live in constantly cold environments have to adapt their metabolism to low temperatures, but mechanisms of enzymatic adaptation to cold environments are not fully understood. Cold active trypsin catalyses reactions more efficiently and binds ligands more strongly in comparison to warm active trypsin. We have addressed this issue by means of comparative free energy calculations studying the binding of positively charged ligands to two trypsin homologues. Stronger inhibition of the cold active trypsin by benzamidine and positively charged P1-variants of BPTI is caused by rather subtle electrostatic effects. The different affinity of benzamidine originates solely from long range interactions, while the increased binding of P1–Lys and –Arg variants of BPTI is attributed to both long and short range effects that are enhanced in the cold active trypsin compared to the warm active counterpart. Electrostatic interactions thus provide an efficient strategy for cold adaptation of trypsin.

Key words: Trypsin; Electrostatics; Binding affinity; Molecular dynamics simulation; Cold adaptation; Psychrophilic enzyme

1. Introduction

Understanding the generally enhanced reaction rates of cold-adapted enzymes often depends on comparison with closely related enzymes working at different temperature [1–4]. Hochachka and Somero [5] suggested that organisms adapted to cold environments need to compensate the reduced temperature by expressing enzymes with increased flexibility in order to maintain a high catalytic efficiency. The increased catalytic efficiency of cold-adapted enzymes would not in general need to be attributed to an overall increase in flexibility, but rather to increased flexibility for some of their structural components [1–3,6]. X-ray analysis of mesophilic (bovine) and psychrophilic (salmon) trypsin did not provide indications of any overall differences in the flexibility [1], though localised weaker interactions between the N- and C-terminal domains were observed in the latter case. Comparative molecular dynamics (MD) simulations of the same two trypsins did not either reveal elevated molecular flexibility of the cold active trypsin [7]. Increased flexibility may, however, not be the only strategy for adaptation to cold environments. Alteration of the electrostatic potential of key residues central to ligand binding and catalysis may also be a strategy for cold adaptation, as seems to be the case for cold active citrate synthase. Cold active citrate synthase has strikingly different electrostatic potential in comparison to its hyperthermophilic counterpart, and focussed electrostatic attraction of substrates has been proposed to be a possible source of the enhanced catalytic efficiency of the cold active citrate synthase [2]. Differences in electrostatic surface potentials in the substrate binding area have also been observed between cold and warm active trypsin (see e.g. [8]), but the effect of this on binding or catalysis is not yet fully understood.

Binding of protein inhibitors, e.g. bovine pancreatic trypsin inhibitor (BPTI), to trypsin is characterised by well defined binding sites, and the binding arrangement closely resembles that of real substrates. The primary specificity of trypsin is to a large extent determined by shape, size and electrostatic potential of the specificity pocket (S1-site). Trypsin has a narrow specificity that predominantly arises from the aspartic acid (Asp^{189}) at the bottom of the specificity pocket. Asp^{189} forms strong electrostatic interactions with complementary charged substrates, whereas the hydrophobic walls of the pocket are capable of forming interactions with the non-polar parts of entering substrates. Recent binding affinity measurements for 18 different P1-variants of BPTI in complex with bovine trypsin (BT) and anionic salmon trypsin (AST) revealed, as expected, a very narrow specificity for cognate Lys and Arg side-chains [9]. The two trypsin homologues bind non-cognate P1-residues at a similar strength, but association constants for AST were 100-fold higher for both cognate P1-variants. Kinetic characterisation of AST and BT showed higher catalytic efficiency (k_{cat}/K_m) for the cold-adapted AST [10], arising from a twofold increase in the k_{cat} and a 10-fold decrease in K_m at 293 K. The water-mediated hydrogen bonding network in the S1-site is highly conserved between BT and AST [1,11], and the binding contacts are virtually identical. This implies that differences in binding affinity and catalytic efficiency between BT and AST arise from sources outside the S1-pocket. Recent Poisson–Boltzmann (PB) calculations [8] indicate that residues outside the S1-pocket cause differences in electrostatic potentials at the S1-site of BT and AST.

In order to investigate the questions raised by Gorfe et al. [8], that electrostatic interactions could be one of the sources to differences in both binding and catalytic features of cold and warm active trypsins, we employ comparative binding free energy calculations. The linear interaction energy (LIE) approach [12] seems to be particular attractive in this respect, and has already proven to be a valuable tool for estimation of

E-mail: bjoerno@chem.uit.no
E-mail: arnes@chem.uit.no
*Corresponding author. Fax: (46)-18-53 69 71.
E-mail: aqvist@xray.bmc.uu.se

0014-5793/01/$20.00
PII: S0014-5793(01)02552-2

Table 1
Average ligand interaction energies within the 16 Å simulation sphere and contribution from distant charges (kcal/mol)

Ligand	$\langle V^{elec}\rangle_{bound}$	$\langle V^{vdW}\rangle_{bound}$	$\langle V^{elec}\rangle_{free}$	$\langle V^{vdW}\rangle_{free}$	$\Delta G^{el}_{long\ range}$	ΔG^{calc}_{bind}	$\Delta\Delta G^{obs\ a}_{bind}$
AST Bza	−111.1	−20.1	−100.6	−9.2	−0.4	−7.6 ± 0.3	−7.1
BT Bza	−111.4	−20.0	−100.6	−9.2	+0.7	−6.6 ± 0.6	−6.3

[a]Experimental data from Os and Otlewski (unpublished).

absolute binding free energies of inhibitor binding to several biological systems [13–17], including trypsin [18,19]. The binding of benzamidine (bza) to trypsin as well as binding of substrate analogues (BPTI) is addressed here by means of comparative MD simulations that form the basis for free energy calculations using the LIE approach.

2. Materials and methods

2.1. The LIE method

The LIE method [12,13] for estimating absolute binding free energies approximates the binding free energy as:

$$\Delta G^{LIE}_{bind} = \alpha\,(\langle V^{vdW}_{l-s}\rangle_{bound} - \langle V^{vdW}_{l-s}\rangle_{free}) + \beta(\langle V^{el}_{l-s}\rangle_{bound} - \langle V^{el}_{l-s}\rangle_{free})$$

where V^{vdW} and V^{el} are the non-polar and the electrostatic interaction energies between the ligand and the surrounding environment respectively, and $\langle\ \rangle$ denotes the ensemble average over a MD simulations trajectory. The electrostatic linear response approximation is used to calculate the polar part of the binding free energy, and the non-polar part is evaluated using an empirical relationship calibrated against a set of experimental binding data. The two coefficients, α and β, are scaling factors for the non-polar and electrostatic contributions to the free energy, respectively. Both of these have been subjected to refinement procedures and here we use the earlier determined values $\alpha = 0.18$ and $\beta = 0.5$ in all calculations [13,20].

2.2. Computational details

MD simulations were carried out starting from the crystal structure of BT-bza (3ptb) and AST-bza (2tbs) [1,21], and the crystal structures of BPTI P1-variants in complex with BT and AST [11,22]. Crystallographic water molecules closer than 12 Å from the simulation centre, defined as the carbon atom of the guanidinium group in bza and the Cα-atom of the P1-residue in BPTI, were included in the calculations. Additional water molecules were added to fill a 16 Å sphere around the simulation centre, and all water molecules were treated with the TIP3P model [23]. Protein atoms outside the 16 Å sphere were highly restrained to their initial positions, and non-bonded interactions across the boundary were excluded. A 10 Å residue-based solute–solute and solute–solvent cut-off was used along with the local reaction field (LRF) method [24]. The LRF method has been shown to reproduce the results of an infinite cut-off at only a modest computational cost, by treating long range electrostatics through a multipole expansion [24]. The non-bonded potentials involving the ligand (bza or the P1-residue) were not subjected to any truncation schemes. Ionisable residues within 12 Å from the simulation centre were considered as charged along with the N-terminal residue, while distant ionisable residues were described using a neutral charge set. The contributions from these charges were taken into account using either a screened Coulombic potential with $\varepsilon = 80$ or the sigmoidal dielectric function of Mehler and Eichele [25]. The total charge of the proteins was zero in the bza calculations, yielding a net charge of +1 for the protein–bza complexes. The protein–protein and solvated BPTI simulations were carried out with a +4 charge within the interaction sphere. The spherical surface of water molecules was subjected to radial and polarisation restraints as defined in [26,27]. Prior to the LIE calculations a stepwise heating procedure followed by a simulation at constant temperature of 300 K was performed for all calculations. Production runs were carried out at 300 K using a time step of 1.5 fs, and the systems were coupled to an external bath [28] to maintain the temperature. Energy data were collected every fifth step. The total length of the simulations ranged from 300 to 450 ps, depending on the time required to reach convergent results. Convergence of the calculated binding free energies was judged by dividing the production phase in two parts, and then calculating a binding free energy for each part. The simulations were defined as converged when the difference between these two binding free energies was less than 1 kcal/mol. This difference was also used as error bars for the calculated binding free energies. All calculations were carried out using the MD program Q [27] with the Amber95 force field [29]. Charges for bza were obtained using the restrained electrostatic potential fitting procedure [30]. Electrostatic potentials were generated through single point quantum mechanical calculations at the Hartree–Fock level with the 6-31G* basis set.

3. Results and discussion

3.1. Simulations of trypsin-bza

Binding of bza to trypsin is characterised by formation of an ion-pair between the positively charged guanidinium group and the negatively charged aspartic acid (Asp^{189}) at the S1-site of trypsin. Bza is also hydrogen-bonded to Ser^{190} and Gly^{219}, as well as to two water molecules. X-ray structures of both AST and BT show that these features are identical in the two structures, and yet the experimental binding free energies shows that binding of bza to AST is about 1 kcal/mol stronger compared to bza-BT (Os and Otlewski, unpublished data). Average ligand surrounding interaction energies for water and protein simulations are presented in Table 1, along with the calculated as well as the experimental binding free energies. It should be noted that the binding free energy of bza to BT has previously been calculated using the LIE approach [18]. Since a different protocol and force field is used in the current work the simulation was recalculated in order to allow a comparison with AST. Without including the contribution from distant charges, the LIE calculations estimate the total binding free energy to −7.3 and −7.2 kcal/mol for binding of bza to BT and AST, respectively. This implies that the electrostatic interactions of the ligand within the primary interaction zone are essentially identical in the cold and warm active trypsin. Average structures from the MD simulations of the two complexes also superimpose remarkably well (Fig. 1), which reflects that the principal interactions are virtually identical. However, the Poisson–Boltzmann (PB) calculations [8] revealed that the electrostatic potential at and around the S1-site was more negative in the AST structure compared to BT (with residues 21, 150, 175, 221B and 224 being important for this difference [8]). The PB calculations also showed that the origins of the differences in potential at the S1-site of the two

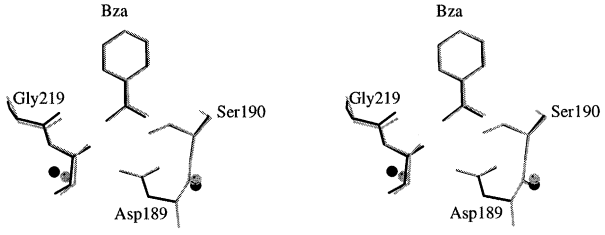

Fig. 1. Superposition of average structures from the MD simulations of bza in complex with bovine (grey) and salmon (black) trypsin.

trypsins was from sources outside the S1-site, and computational modelling of the host–ligand energetics requires treatment also of the long range electrostatic interactions. The LIE calculations were as mentioned, performed with a +1 charge in the 16 Å sphere keeping distant ionisable residues neutral. This procedure does, however, requires a correction term to be added to the final binding free energy to account for the neglected distant charges. Since all such charges are located on the protein surface their electrostatic effects will be screened by a high dielectric constant (the assignment of protonation states of surface charges at the relevant pH [9], is in this case straightforward). It has been shown that three alternative ways of estimating long range electrostatic effects, namely (1) Coulomb's law with a high dielectric constant, (2) the Mehler and Eichele function and (3) the PB equation, all are able to reproduce the experimental data pertaining to the interactions of distant charges with the active site in subtilisin [31]. Using a Coulombic potential with $\varepsilon = 80$, the total binding free energies become -6.6 ± 0.6 and -7.6 ± 0.3 kcal/mol for binding of bza to BT and AST, respectively. Evaluation of the long range contribution using the sigmoidal screening function of Mehler and Eichele [25] yields very similar results (0.1–0.2 kcal/mol difference) to the screened Coulombic potential. Furthermore, the calculated binding free energies can be divided into electrostatic and non-polar contributions, and Table 1 shows that the non-polar contribution is identical in the two complexes and amounts to −2.0 kcal/mol. Based on these arguments, differences in binding of bza to BT and AST are caused by dissimilar long range electrostatic interactions that arise from charged groups located outside the binding site.

3.2. Protein–protein simulations

X-ray analysis [22] has shown that interactions from the secondary binding contacts in the complexes between P1-variants of BPTI and trypsin is virtually identical, and that the binding free energy difference $\Delta G_X - \Delta G_{Gly}$ can be used as a measure of the strength of the interaction formed between the P1–X side-chain and the S1-site of trypsin. The idea is then to treat the P1-residue as 'ligand' in the LIE calculations, and to calculate the contribution from the P1–X side-chain to the total binding free energy by subtracting the P1–Gly interactions. The reference state will thus be the P1–Gly variant. Unfortunately, the experimental structure of the P1–Gly complex is only available for BT. The experimental association measurements [9] showed that the contribution to the association energy that arises from secondary interactions is similar in the P1–Gly complexes (BT and AST). Furthermore, the P1–Gly residue does not have a side-chain that interacts with the S1-site in the complex, and it is therefore assumed that the difference in association energy of P1–Gly to AST and BT is not caused by the P1-residue itself. Comparison of the electrostatic potentials of the two trypsins showed that the AST surface is overall more negative [8], and it is hence reasonable to expect that long range electrostatic interactions are the source of the different affinity of P1–Gly as BPTI is positively charged (+6 charge). Based on these arguments, the reference state for the calculations involving both AST and BT is chosen to be the P1–Gly from BT.

Association measurements [9] revealed an approximately 100 times stronger association of BPTI P1–Lys in complex with AST compared to BT, corresponding to about 2.2 kcal/mol. The calculated average P1–Lys interaction energies in the complex as well as in solvated BPTI are presented in Table 2 for BT and AST, along with the P1–Gly interactions. The experimental association energy measurements showed that the contribution from the P1–Lys side-chain to the total association energy is −12.3 and −14.5 kcal/mol for BT and AST, respectively, whereas the LIE calculations yield -12.3 ± 0.8 and -15.0 ± 0.4 kcal/mol (Table 3) after correction for neglect of distant charges. The contribution from distant charges is also in this case approximated using a Coulombic potential with $\varepsilon = 80$, and the sigmoidal screening function again yields a correction that is 0.1–0.2 kcal/mol more positive than the Coulombic. Table 2 also shows that the non-polar contribution is identical in the two complexes, while the electrostatic part is 2.5 kcal/mol more favourable in the AST complex. Thus, also for BPTI binding the difference in affinity between the two trypsins is caused by different electrostatic interactions.

Table 2
Average ligand interaction energies and long range binding contributions (kcal/mol)

Ligand	$\langle V^{elec} \rangle$	$\langle V^{vdW} \rangle$	$\Delta G^{el}_{long\ range}$
AST P1–Arg	−130.2	−23.4	−0.2
AST P1–Lys	−136.8	−20.8	−0.2
BT P1–Arg	−127.7	−23.9	+0.8
BT P1–Lys	−133.8	−20.7	+0.8
BT P1–Gly	−90.8	−5.1	
BPTI P1–Arg	−112.8	−11.0	+0.6
BPTI P1–Lys	−121.3	−8.6	+0.6
BPTI P1–Gly	−99.9	−3.3	

Binding of P1–Arg to trypsin is the strongest of all P1-variants with an association energy of −18.4 and −20.8 kcal/mol, and subtraction of the contribution from secondary binding sites (P1–Gly) yields a P1–S1 interaction free energy of −12.8 and −15.2 kcal/mol for BT and AST, respectively. Experimental structures are not available for either of the complexes, and models were built based on the respective P1–Lys complexes. The complexity of the water-mediated hydrogen bonding network at the S1-site changes in response to size, charge and shape of the P1-residue accommodated at the S1-site [22]. It is of crucial importance to maintain a saturated hydrogen bonding pattern when the ligand/P1-residue is carrying a net charge or is highly polar. This is related to the fact that burial of charges is generally thermodynamically unfavourable, unless they can acquire sufficiently favourable interactions. Binding of both polar and ionic ligands must therefore be accompanied by a local stabilisation, which is achieved through specific hydrogen bonding interactions. Additional information regarding the internal water structure around the ion-pair interaction formed between the P1-residue and

Table 3
Calculated and observed binding free energies relative to BT P1–Gly (kcal/mol)

Ligand	$\Delta\Delta G^{calc}_{bind}$ [a]	$\Delta\Delta G^{obs}_{bind}$ [b]
AST P1–Arg	-16.0 ± 0.4	−15.2
AST P1–Lys	-15.0 ± 0.4	−14.5
BT P1–Arg	-13.7 ± 0.5	−12.8
BT P1–Lys	-12.3 ± 0.8	−12.3

[a] Calculated based on data from Table 2.
[b] Experimental values from [9].

Asp^{189} was obtained from the X-ray structures of trypsin in complex with bza [1]. This was primarily motivated by the fact that the guanidinium group of bza and the P1–Arg side-chains should overlap in the complexes. The LIE calculations estimate the binding free energy associated with accommodation of P1–Arg at the S1-site to -13.7 ± 0.5 and -16.0 ± 0.4 kcal/mol (including the contribution from distant charges) for BT and AST (Table 3). The more negative value of AST is once more caused by a stronger electrostatic contribution (Table 2), and the non-polar contribution to the binding free energy is again identical in the two trypsins.

Even though the calculated binding free energies reproduce the experimental association measurements in a quantitative manner, questions regarding structural differences within the MD simulations should be examined carefully. Such issues must thus be addressed in order to both validate the MD simulations and to rule out the possibility that structural differences are responsible for the elevated inhibition of AST. The average structure from the MD simulations of P1–Lys and P1–Arg in complex with AST has been superimposed on the corresponding complexes of BT (Figs. 2 and 3). The average structure from the two bza simulations (Fig. 1) showed that the principal interactions between bza and the substrate binding site were identical in the two structures. Figs. 2 and 3 reveal that the binding arrangement involving the P1-side-chain is also very similar in the BT and AST simulations, but the difference in affinity of P1–Lys/Arg between AST and BT is not solely caused by long range electrostatics. However, the non-polar part of the P1–S1 interaction is the same in accommodation of both variants, and the difference in affinity is entirely due to electrostatic interactions.

3.3. Electrostatic effects on binding and catalysis

It is well recognised that the speed of chemical reactions is temperature dependent, and that decreased temperatures generally lower reaction rates. Cold-adapted enzymes are therefore faced with the problem of maintaining sufficient catalytic speed to ensure a functional metabolism at low temperatures. This obviously requires adaptational strategies that must be developed through evolution of the catalytic systems to counteract the temperature problem. Attractive electrostatic interactions are formed exothermically and are stabilised at lower temperatures, in contrast to endothermically formed non-polar interactions that are destabilised at lower temperatures. The strength of the interactions plays a crucial role in this context, and electrostatic interactions are expected to have a more important function than non-polar interactions due to their long range nature. In fact, we find that they are the dominant contribution to the association energy in binding

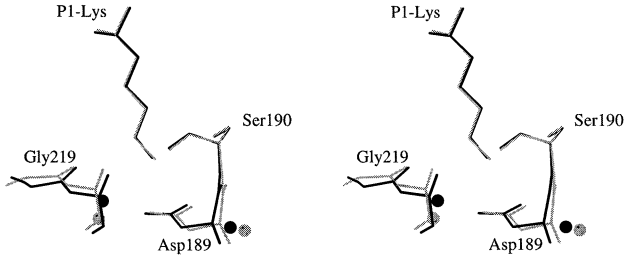

Fig. 2. Superposition of average structures from the MD simulations of BPTI P1–Lys in complex with bovine (grey) and salmon (black) trypsin.

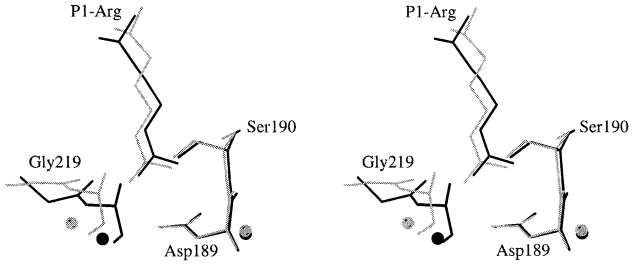

Fig. 3. Superposition of average structures from the MD simulations of BPTI P1–Arg in complex with bovine (grey) and salmon (black) trypsin.

of positively charged ligands to both cold (AST) and warm (BT) active trypsin. This effect is even more pronounced in the cold active trypsin, as is clearly demonstrated by the present calculations. Thus, positively charged inhibitors bind significantly more strongly to the cold active AST due to enhanced electrostatic interactions in comparison to the warm active BT.

Kinetic characterisation of AST and BT showed a notably reduced K_m, and slightly increased k_{cat} for AST [10]. The rate determining step in hydrolysis of amides is, according to the standard serine proteinase mechanism [32], the acylation process. The measured K_m and k_{cat} should therefore approximate the true binding affinity (K_s) and acylation rates (k_2), and increased catalytic efficiency for the cold active AST is consequently to a large extent a result of higher binding affinity. Based on the comparative binding free energy calculations presented here, increased binding affinity of AST is caused by optimisation of electrostatic features. This is a different origin than the previously proposed flexibility hypothesis. Hence, it is reasonable to expect that the decrease in K_m is also caused by the enhanced electrostatic potential that in turn results in a tighter binding. This is also further supported by the fact that the binding arrangement of the BPTI–trypsin complexes closely resembles that of real substrates.

Acknowledgements: This work was supported by grants from the Swedish Research council to J.Å., and the Norwegian Research council to A.O.S. B.O.B. gratefully acknowledges support from NorFa.

References

[1] Smalås, A.O., Heimstad, E.S., Hordvik, A., Willassen, N.P. and Male, R. (1994) Proteins 20, 149–166.
[2] Russell, R.J., Gerike, U., Danson, M.J., Hough, D.W. and Taylor, G.L. (1998) Structure 6, 351–361.
[3] Bentahir, M., Feller, G., Aittaleb, M., Lamotte-Brasseur, J., Himri, T., Chessa, J.P. and Gerday, C. (2000) J. Biol. Chem. 275, 11147–11153.
[4] Smalås, A.O., Leiros, H.K., Os, V. and Willassen, N.P. (2000) Biotechnol. Annu. Rev. 6, 1–57.
[5] Hochachka, P.W. and Somero, G.N. (1984) Biochemical adaptations, Chapter 11, Princeton University Press, Princeton, NJ.
[6] Fields, P.A. and Somero, G.N. (1998) Proc. Natl. Acad. Sci. USA 95, 11476–11481.
[7] Brandsdal, B.O., Heimstad, E.S., Sylte, I. and Smalås, A.O. (1999) J. Biomol. Struct. Dyn. 17, 493–506.
[8] Gorfe, A.A., Brandsdal, B.O., Leiros, H.K., Helland, R. and Smalås, A.O. (2000) Proteins 40, 207–217.
[9] Krowarsch, D., Dadlez, M., Buczek, O., Krokoszynska, I., Smalås, A.O. and Otlewski, J. (1999) J. Mol. Biol. 289, 175–186.

[10] Outzen, H., Berglund, G.I., Smalas, A.O. and Willassen, N.P. (1996) Comp. Biochem. Physiol. B 115, 33–45.
[11] Helland, R., Leiros, I., Berglund, G.I., Willassen, N.P. and Smalås, A.O. (1998) Eur. J. Biochem. 256, 317–324.
[12] Åqvist, J., Medina, C. and Samuelsson, J.E. (1994) Protein Eng. 7, 385–391.
[13] Hansson, T., Marelius, J. and Åqvist, J. (1998) J. Comput.-Aided Mol. Des. 12, 27–35.
[14] Lamb, M.L., Tirado-Rives, J. and Jorgensen, W.L. (1999) Bioorg. Med. Chem. 7, 851–860.
[15] Gorse, A.D. and Gready, J.E. (1997) Protein Eng. 10, 23–30.
[16] Wall, I.D., Leach, A.R., Salt, D.W., Ford, M.G. and Essex, J.W. (1999) J. Med. Chem. 42, 5142–5152.
[17] Paulsen, M.D. and Ornstein, R.L. (1996) Protein Eng. 9, 567–571.
[18] Åqvist, J. (1996) J. Comput. Chem. 17, 1587–1597.
[19] Brandsdal, B.O., Åqvist, J. and Smalås, A.O. (2001) Protein Sci., in press.
[20] Marelius, J., Hansson, T. and Åqvist, J. (1998) Int. J. Quant. Chem. 69, 77–88.
[21] Marquart, M., Walter, J., Deisenhofer, J., Bode, W. and Huber, R. (1983) Acta. Cryst. B B39, 480–490.
[22] Helland, R., Otlewski, J., Sundheim, O., Dadlez, M. and Smalås, A.O. (1999) J. Mol. Biol. 287, 923–942.
[23] Jorgensen, W.L., Chandrasekhar, J., Madura, J.D., Impey, R.W. and Klein, M.L. (1983) J. Chem. Phys. 79, 926–935.
[24] Lee, F.S. and Warshel, A. (1992) J. Chem. Phys. 97, 3100–3107.
[25] Mehler, E.L. and Eichele, E. (1984) Biochemistry 23, 3887–3891.
[26] King, G. and Warshel, A. (1989) J. Chem. Phys. 91, 3647–3661.
[27] Marelius, J., Kolmodin, K., Feierberg, I. and Åqvist, J. (1998) J. Mol. Graph. Model. 16, 213–225.
[28] Berendsen, H.J.C., Postma, J.P.M., van Gunsteren, W.F., di Nola, A. and Haak, J.R. (1984) J. Chem. Phys. 81, 3684–3690.
[29] Cornell, W.D., Cieplak, P., Bayly, C.I., Gould, I.R., Merz Jr, K.M., Ferguson, D.M., Spellmeyer, D.C., Fox, T., Caldwell, J.W. and Kollman, P.A. (1995) J. Am. Chem. Soc. 117, 5179–5197.
[30] Bayly, C.I., Cieplak, P., Cornell, W.D. and Kollman, P.A. (1993) J. Phys. Chem. 97, 10269–10280.
[31] Sternberg, M.J., Hayes, F.R., Russell, A.J., Thomas, P.G. and Fersht, A.R. (1987) Nature 330, 86–88.
[32] Zerner, B. and Bender, M.L. (1964) J. Am. Chem. Soc. 86, 3669–3674.